α decay of ^{176}Au

A. N. Andreyev,[1,2] S. Antalic,[3] D. Ackermann,[4] T. E. Cocolios,[5] J. Elseviers,[6] S. Franchoo,[7] S. Heinz,[4] F. P. Heßberger,[4,8] S. Hofmann,[4,9] M. Huyse,[6] J. Khuyagbaatar,[4] B. Kindler,[4] B. Lommel,[4] R. Mann,[4] R. D. Page,[10] P. Van Duppen,[6] and M. Venhart[6]

[1]*Department of Physics, University of York, YO10 5DD, United Kingdom*
[2]*Advanced Science Research Centre, Japan Atomic Energy Agency, Tokai-mura, 319-1195, Japan*
[3]*Department of Nuclear Physics and Biophysics, Comenius University, Bratislava, 84248, Slovakia*
[4]*GSI Helmholtzzentrum für Schwerionenforschung GmbH, 64291 Darmstadt, Germany*
[5]*University of Manchester, Manchester M13 9PL, United Kingdom*
[6]*KU Leuven, Instituut voor Kern- en Stralingsfysica, B-3001 Leuven, Belgium*
[7]*IPN Orsay, F-91406 Orsay Cedex, France*
[8]*Helmholtz Institut Mainz, 55099 Mainz, Germany*
[9]*J.W. Goethe-Universität, D-60054 Frankfurt, Germany*
[10]*Department of Physics, Oliver Lodge Laboratory, University of Liverpool, Liverpool L69 7ZE, United Kingdom*

(Received 21 August 2014; revised manuscript received 25 September 2014; published 16 October 2014)

The isotope ^{176}Au has been studied in the complete fusion reaction ^{40}Ca + ^{141}Pr $\rightarrow$ ^{176}Au + 5n at the velocity filter SHIP (GSI, Darmstadt). The complex fine-structure α decay of two isomeric states in ^{176}Au feeding several previously unknown excited states in the daughter nucleus ^{172}Ir is presented. An α-decay branching ratio of $b_\alpha = 9.5(11)\%$ was deduced for the high-spin isomer in ^{172}Ir.

DOI: 10.1103/PhysRevC.90.044312 PACS number(s): 23.60.+e, 25.70.−z, 27.70.+q

I. INTRODUCTION

Studies of odd-odd nuclei are notoriously difficult as generally known, both theoretically [1] and experimentally [2]. This is partially because the coupling of the odd valence neutron and proton may result in multiplets of low-lying states, some members of which can become isomeric. Often a relatively small energy spacing between the multiplet states strongly complicates the experimental studies. The study of such states is important as it provides information on the proton-neutron interaction involved in the different configurations. In this respect α decay offers an ideal tool to selectively identify the states in the daughter nucleus with the same spin, parity, and configuration as in the α-decaying parent.

The present paper reports on a detailed α-decay investigation of the very neutron-deficient nucleus ^{176}Au ($Z = 79$, $N = 97$). The nuclide is situated in the transitional region between possibly weakly deformed or triaxial isotopes ^{177,179}Au on the one hand and presumably nearly spherical isotopes ^{171,173,175}Au on the other, see, e.g., [3]. Therefore, the studies of ^{176}Au could provide further insights on nuclear structure changes in this region of nuclei. This isotope was previously studied in several experiments [4–8], for consistency of the discussion, Table I collates all published α-decay data for ^{176}Au and its daughter ^{172}Ir [9], while our results are given in Table II. In all previous experiments at most several thousands of α decays of ^{176}Au were registered. As shown in the present work, measuring solely α decays is insufficient as ^{176}Au has a complex α-decay pattern which only can be disentangled when α-γ coincidence measurement are employed. This technique was used in the as yet unpublished study of ^{176}Au [7] at the Fragment Mass Analyzer (FMA), but this work also suffered from insufficient statistics, due to which only the strongest fine-structure α decays of ^{176}Au could be identified. Nevertheless, this was the first study which proposed two α-decaying states in this nucleus with tentative spin-parity assignments of (9^+) and (3^-). It also identified two groups of α-γ coincidences of α(6080 keV)-γ(212 keV) and α(6117 keV)-γ(175 keV), originating from presumed (9^+) state, see Table I. In the most recent study at FMA [8], ^{176}Au was produced as a daughter of ^{180}Tl after its α decay. Due to this specific production method, the authors observed the decay of only one state in ^{176}Au, which they denoted as the 'ground state' with a tentative spin assignment of $I^\pi = (4^-)$, see Table I. The decay properties of this state are similar to that of the (3^-) state observed in [7], though the tentative spin assignment is different. To our knowledge, the relative excitation energy of the two α-decaying states is still unknown, therefore we will denote them throughout our work as the high-spin and low-spin isomeric states, ^{176}Au^{hs} and ^{176}Au^{ls}, respectively, see Table I.

In our experiment at the velocity filter SHIP at GSI in Darmstadt [10], we collected $\sim 1.6 \times 10^5 \alpha$ decays of ^{176}Au. This is at least an order of magnitude larger than in any previous study, which allowed us to perform a detailed α-γ decay investigation of both isomeric states in ^{176}Au. We mention already now that for the interpretation of some of our results we used the unpublished half-lives of two isomeric states in ^{176}Au from the work [7], along with the results of a complementary α-decay investigation of ^{180}Tl from study [11].

II. EXPERIMENTAL SET UP

The isotope ^{176}Au was produced in the complete-fusion reaction ^{40}Ca + ^{141}Pr $\rightarrow$ ^{176}Au + 5n. The typical intensity of the ^{40}Ca beam, provided by the UNILAC of GSI, was 600 pnA. The UNILAC macropulse had a total duration of 20 ms with a time structure of 5 ms "beam on" followed by a 15 ms "beam off" interval.

TABLE I. α-decay energies E_α (coincident E_γ, if observed), branching ratios b_α, half-life values $T_{1/2}$, relative intensities I_α, and tentative spin assignments I^π (when proposed) for ^{176}Au and its daughter ^{172}Ir as quoted by the earlier studies.

Isotope, I^π	b_α(%)	E_α (keV); coinc. E_γ (keV)	$T_{1/2}$ (s)	I_α (%)	Ref.
^{176}Au		6.26(1)	1.25(30)	∼80	[4]
		6.29(1)		∼20	
^{176}Au		6228(10)			[5]
		6282(10)			
^{176}Au		6286	$0.84^{+0.17}_{-0.14}$		[6]
		6260			
^{176}Au^{hs}, (9^+)		6080(5); γ(212.0)	1.36(2)	26(2)	[7]
		6117(5); γ(175.0)		49(3)	
		[6220(5)][a]; (Ir K x rays)		21(2)	
		(6287)[b]		<4	
^{176}Au^{ls}, (3^-)		6282(5)	1.05(1)	100	
^{176}Au^{ls}, (4^-)	75(8)	6294(10)	1.2(4)	100	[8]
^{172}Ir^{hs}, (7^+)	23(3)	5828	2.0(1)	100	[9]
^{172}Ir^{ls}, (3^+)	2	5510(10)	4.4(3)	100	

[a]Tentatively explained as the summing α + electron line [7].
[b]A weak line, tentatively proposed as the summing α + electron line [7].

Eight ^{141}Pr targets (100% natural isotopic abundance), each of 350 μg/cm^2 thickness, were mounted on a wheel, rotating synchronously with the UNILAC macropulsing. The targets were produced by evaporating the $^{141}PrF_3$ material onto a carbon backing of 40 μg/cm^2 thickness. Data were taken at the two beam energies of 208 and 212 MeV in front of the target, covering the expected maximum of the 5*n* evaporation channel for the studied reaction.

After separation by SHIP, the evaporation residues (ERs) were implanted into a 300 μm thick, 35×80 mm^2 16-strip position-sensitive silicon strip detector (PSSD), where their subsequent α decays were measured by using standard implantation and correlation techniques [12]. For the PSSD energy calibration we used known α-decay lines of the isotopes $^{176-182}$Hg (and their daughters), produced in the ^{40}Ca + ^{144}Sm $\rightarrow$ ^{184}Pb* reaction, which was studied in the same experiment prior to the irradiation of the ^{141}Pr target. A typical PSSD energy resolution of ∼25 keV (FWHM) was achieved in the energy interval of 6000–6500 keV.

A large-volume four-crystal Clover germanium detector was installed behind the PSSD to measure the energies of γ rays detected within 5 μs of the detection of any particle or fission decay in the PSSD. Its performance and γ-ray efficiency for experiments at SHIP were described in [13]. A time-analog-converter (TAC) was used to measure the time difference between the particle and γ decay. The energy threshold for the γ-ray registration was at ∼20 keV, therefore we could not observe Au and Ir *L* x rays in this experiment.

Three time-of-flight (TOF) detectors [14] were installed in front of the PSSD allowing us to distinguish the reaction products from the scattered beam particles. In addition, decay events in the PSSD could be distinguished from the implantation events by requiring an anticoincidence condition between the signals from the PSSD and at least one of the TOF detectors.

Due to a relatively high recoil implantation rate in the PSSD (∼1 kHz) and relatively long half-lives of the isotopes of interest, the half-life measurements both for ^{176}Au and for its neighbors and daughter products could not be determined using ER–α-decay correlations, usually applied in implantation experiments. Therefore, the isotope identification was performed based on Q_α-value arguments, on the α-γ analysis and on the α-α correlation analysis.

TABLE II. α-decay energies E_α, coincident γ rays, relative intensities $I_{rel,\alpha}$, reduced α-decay widths δ^2_α, relative hindrance factors HF_{rel} and total $Q_{\alpha,tot} = Q_\alpha + E_\gamma$ values, deduced in our work for ^{176}Au. To calculate the reduced α-decay widths for ^{176}Au^{ls}, an α-branching ratio of 75(8)% from [8] was used, while $b_\alpha = 100\%$ was assumed for the high-spin isomer in ^{176}Au.

Isomer, I^π	E_α, keV	E_γ, keV	$I_{rel,\alpha}$, %	δ^2_α, keV	HF_{rel}	$Q_{\alpha,tot}$, keV
^{176}Au^{hs}	6082(7)	211.6(3)	26(5)	43(9)	1.8(4)	6435(7)
	6117(7)	175.2(3)	66(5)	79(8)	1	6434(7)
	6287(7)		8(1)	2.0(3)	40(6)	6433(7)
^{176}Au^{ls}	5798(20)	500.0(6)	<0.4	<10.3(23)	>2.4	6433(20)
	6054(20)	236.6(3)	<1	<2.1(5)	>12	6432(20)
	6138(15)	151.5(3)	<5	<4.8(9)	>5.2	6433(15)
	6157(20)	126.3(3)	<2	<1.6(3)	> 15.7	6426(20)
	6287(7)		100	25(3)	1	6433(7)

III. EXPERIMENTAL RESULTS

A. α-γ and α-α correlation analysis for ^{176}Au

1. α-γ analysis for ^{176}Au

Figure 1(a) shows a part of the total energy spectrum of α decays collected during the "beam off" time intervals at both beam energies used in the experiment. The strongest peaks in the spectrum are due to known α decays of the isotopes ^{175}Pt [5959(5) keV], ^{177}Au^{m} [6124(7) keV], and ^{177}Au^{g} [6161(7) keV] [3,15] produced in different evaporation channels of the studied reaction. The measured α-decay energies of all mentioned isotopes are in a good agreement with the previously known data.

The two peaks at 6222(20) keV and 6287(7) keV have energies similar to those reported for ^{176}Au by the earlier studies, in particular in the most detailed work to date [7], see Table I. However, we will unambiguously prove that the former peak is due to the known effect of α particle-conversion electron energy summing in the PSSD [17,18], thus it does not represent a real α decay of ^{176}Au. The same conclusion was tentatively proposed in [7]. Other known and also new weak α decays, identified in our work for ^{176}Au, are masked in Fig. 1(a) by the much stronger α decays of ^{177}Au. These decays of ^{176}Au were established from α-γ coincidences as shown in Fig. 1(b). A few known groups of α-γ events are marked in the spectrum with their corresponding γ decay energies, including the groups at α(5959 keV)-γ(77 keV) and α(5959 keV)-Os K x rays, which are due to the fine-structure α decay of ^{175}Pt [15]. The group α[5828(10) keV]-γ(162.1 keV), relevant for the following discussion, represents the decay of the high-spin isomer ^{172}Ir^{hs}.

The projections on the E_γ axis from the two regions of Fig. 1(b), marked by 'A' (a rectangular region) and 'B' (a 'sloped' parallelogram region) are shown in Figs. 2(a) and 2(b), respectively. As shown below, the 'sloped' shape for the region 'B' enhances the identification of weaker fine-structure α decays of ^{176}Au. We note the presence of strong Ir $K_{\alpha,\beta}$

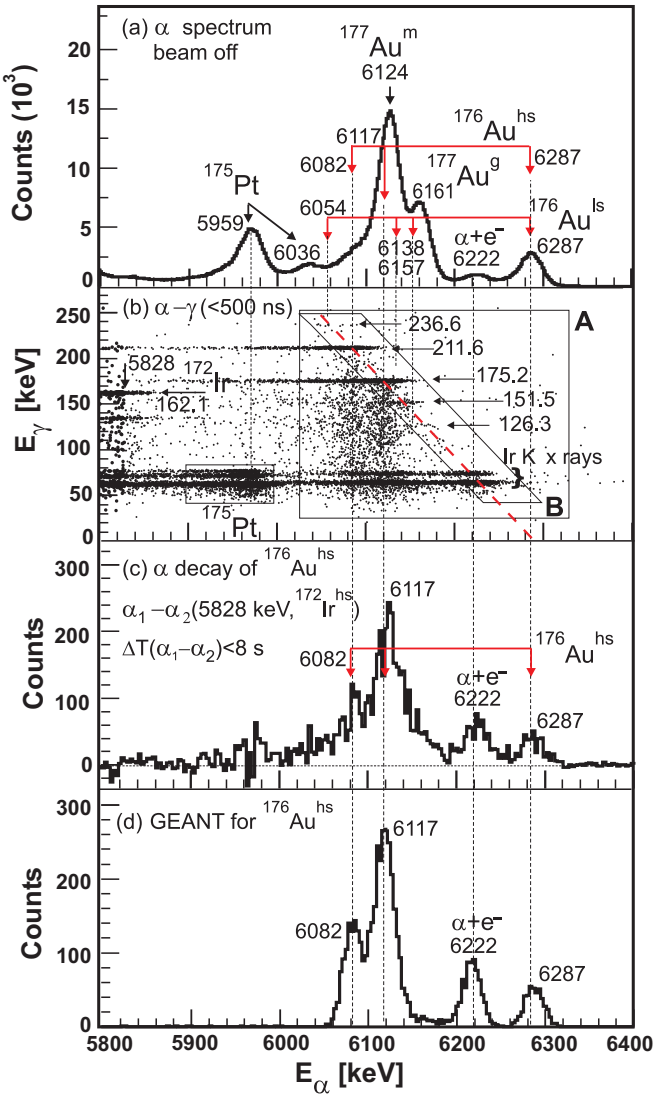

FIG. 1. (Color online) (a) Part of the α-decay energy spectrum from the reaction ^{40}Ca + ^{141}Pr → ^{181}Au* registered during the "beam off" intervals in the PSSD. The red arrows indicate the positions of the α decays assigned by us to the decay of the high- and low-spin isomers in ^{176}Au. All energies are given in keV. (b) The E_α-E_γ coincidence spectrum for α events from (a) measured within the time interval of $\Delta T(\alpha\text{-}\gamma) \leqslant 500$ ns. The red dashed line corresponds to the constant value of $Q_{\alpha,\mathrm{tot}} = 6434$ keV, see text. (c) Random-background subtracted spectrum of α decays of ^{176}Au correlated with the 5828 keV α decay of ^{172}Ir^{hs} within the time interval of $\Delta T(\alpha - \alpha) \leqslant 8$ s, data both from "beam on" and "beam off" intervals. (d) The results of the GEANT simulations for the α decay of ^{176}Au^{hs}, see details in the text.

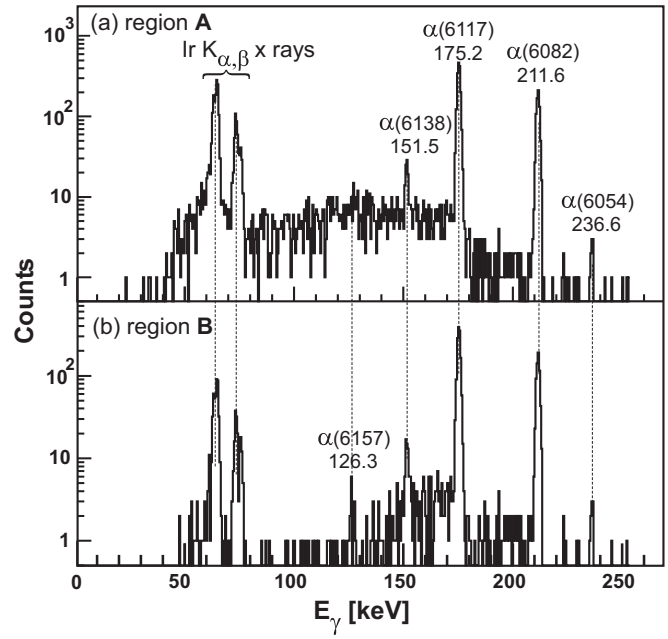

FIG. 2. (a) Projection on the E_γ axis of the events from the region 'A' of Fig. 1(b). (b) The same for the 'sloped' region 'B' of Fig. 1(b). Relevant peaks are labeled with the energy of the α decay of ^{176}Au (top line) feeding to the respective excited state in ^{172}Ir and the energy of the coincident γ ray (bottom line). All energies are given in keV.

x rays in Figs. 1(b) and 2 at the measured energies of 63.3(3), 64.8(3), 73.4(3), and 75.6(3) keV, which agree well with the tabulated values [19].

The analysis of Figs. 1(b) and 2 allowed us to identify five groups of coincident α-γ events: 6157(20)–126.3(3) keV, 6138(15)–151.5(3) keV, 6117(7)–175.2(3) keV, 6082(7)–211.6(3) keV, and 6054(20)–236.6(3) keV. Additionally, a sixth group of four α[5798(20) keV]-γ[500.0(5) keV] events (not shown in the spectra), was observed in this analysis. The groups at 6117–175 keV and 6080–212 keV were previously seen in study [7] and were assigned to the decay of ^{176}Au^{hs}.

The total $Q_{\alpha,tot} = Q_\alpha + E_\gamma$ values for these six groups agree well to each other within the experimental uncertainty, see Table II. To further highlight this fact, the red dashed line was drawn in Fig. 1(b), which corresponds to the constant value of $Q_{\alpha,tot} = 6434$ keV, deduced for the 6117–175.2 keV and 6082–211.6 keV decays, being the two strongest for ^{176}Au.

The 126.3, 151.5, 236.3, and 500.0 keV γ rays have intensities at least an order of magnitude lower than the 175.2 and 211.6 keV γ rays, see Fig. 2. This fact, along with at least an order of magnitude lower statistics for ^{176}Au in work [7] in comparison to our study, readily explains the nonobservation of these weak decays in the earlier experiment.

Based both on the $Q_{\alpha,tot}$-value argument and on the discussion in the following sections, all six groups were assigned to the decay of ^{176}Au. This is because all neighboring Au and Pt nuclei and their daughter products, except for the weakly produced ^{175}Au, have their Q_α values lower than the $Q_{\alpha,tot}(^{176}\text{Au}) = 6434$ keV. Furthermore, both the much lower production of ^{175}Au and its higher value of $Q_\alpha(^{175}\text{Au}) = 6583(7)$ keV exclude this isotope as being the source of any of the decays in Table II.

2. *Complementary data for ^{180}Tl → ^{176}Au decay from study at ISOLDE*

Based on the same $Q_{\alpha,tot}$ value for all six groups, one is tempted to assign all of them as originating from the high-spin isomer in ^{176}Au, from which the 6117–175 keV and 6082–212 keV decays proceed. However, we will show in this section, that all newly identified groups must be due to the fine-structure α decay of the low-spin isomer ^{176}Au, see Fig. 3 and Table II.

This inference is based on complementary α-decay data for the isotope ^{180}Tl from our dedicated high-statistics β decay and β-delayed fission study [20–22] at the mass separator ISOLDE. While the detailed analysis of α-decay data for ^{180}Tl is given elsewhere [11], here we will only provide the data relevant for the present discussion of ^{176}Au. Namely, in the study of ^{180}Tl at ISOLDE, approximately $1.4 \times 10^6 \alpha$ decays of ^{180}Tl were observed, which is at least two orders of magnitude larger than in any previous study of this nucleus, including the latest FMA work [8]. Furthermore, by using the selective Resonance Ionization Laser Ion Source (RILIS) of ISOLDE, a pure source of ^{180}Tl was obtained. This allowed us to perform a unique simultaneous α-decay study of ^{180}Tl and of its daughter product ^{176}Au.

For the following discussion, we remind that the ground state of ^{180}Tl has a half-life of 1.09(1) s and a tentative spin-parity assignment of $(4^-,5^-)$ as proposed by our studies [20–22] or (5^-) in Ref. [8]. No evidence for the existence of another α- or β-decaying isomer was found. This alone strongly suggests that the α decay of ^{180}Tl should selectively populate only the lower-spin isomer in ^{176}Au. This was indeed confirmed by the nonobservation of the 6082–211.6 keV and/or 6117–175.2 keV decays of the high-spin isomer in ^{176}Au^{hs}. In contrast to this, in the ISOLDE experiment, we clearly observed the groups at 6157–126.3(3) keV, 6138–151.5(3) keV, 6054–236.6(3) keV, and 5798 keV)–γ(500.0(5) keV, apparently the same as in the present study of ^{176}Au at SHIP.

The above-mentioned facts prove that the two isomeric states in ^{176}Au have different α-decay patterns. The presumed high-spin 1.36-s isomer of ^{176}Au decays by the 6082–211.6 keV, 6117–175.2 keV, and by the 6287(7) keV crossover transitions (see below) all of them seen in the present study and in the work [7], see Fig. 3.

On the other hand, the 6157(20)–126.3(3) keV, 6138(15)–151.5(3) keV, 6054(20)–236.6(3) keV, 5798(20)–500.0(5) keV, and the 6287(7) keV crossover decay must be associated with the decay of the low-spin 1.05-s isomer in ^{176}Au, proposed by [7]. As will be shown below, despite the highest-energy α decays of both ^{176}Au^{hs,ls} having the same energy of 6287 keV, their presence and relative intensities can be reliably established from the SHIP data.

3. *α_1(^{176}Au^{hs,ls})–α_2(^{172}Ir^{hs,ls}) correlation analysis*

We now return to the data measured for ^{176}Au at SHIP and consider the decays of two isomeric states separately. As the next step, we performed the $\alpha_1(^{176}\text{Au})$–$\alpha_2$(5828 keV, ^{172}Ir^{hs}) correlation analysis, by searching for α decays of the parent isotope ^{176}Au in correlations with the 5828 keV α decay of the presumed high-spin isomer of the daughter nucleus ^{172}Ir [$T_{1/2} = 2.0(1)$ s]. A time interval of $\Delta T(\alpha_1\text{-}\alpha_2) \leqslant 8$ s was applied in the analysis. Both due to the high rate of recoil implantations and α decays in the PSSD, and a relatively long time range for the correlation search, the resulting spectrum of the parent α_1 decays becomes swamped with random correlations. That is why Fig. 1(c) shows the background-subtracted spectrum of the parent α_1 decays from the α_1(5800–6400 keV)–α_2(5828 keV, ^{172}Ir^{hs}) correlations analysis. As a "background" spectrum a random spectrum of α_2 decays was used, produced from the the "reciprocal" α_1(5828 keV,^{172}Ir^{hs}) -α_2(5800–6400 keV) correlation analysis, which has no true correlations within the selected energy regions. The same time condition of 8 s was used in this analysis. The validity of this method is confirmed by the disappearance in Fig. 1(c) of the 5959 keV α decay of ^{175}Pt [which is present in Fig. 1(a)], as indeed it cannot have correlations with the 5828 keV α decay.

Clearly, due to the condition of correlations with the 5828 keV decay of ^{172}Ir^{hs}, the α peaks in Fig. 1(c) at 6082, 6117, 6222, and 6287 keV must be solely due to ^{176}Au^{hs}, with no admixture from ^{176}Au^{ls} or any other nuclides.

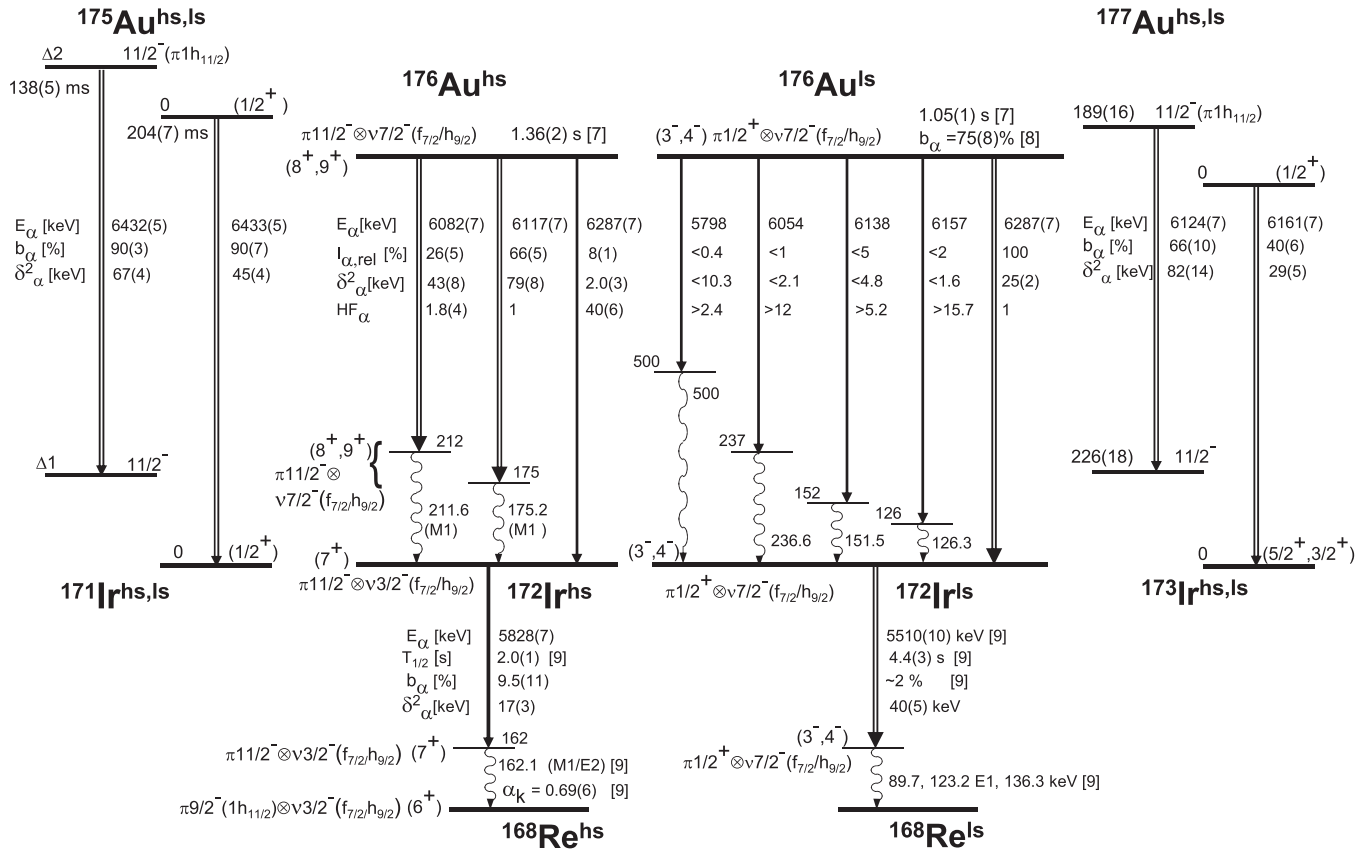

FIG. 3. Decay schemes of ^{176}Au^{hs,ls} deduced in our work, see text and Table II for details. Shown are α-decay energies E_α, relative intensities $I_{\alpha,rel}$, reduced α-decay widths δ^2_α, and hindrance factor values HF$_\alpha$. The hindrance factors HF$_\alpha$ for ^{176}Au^{hs} and ^{176}Au^{ls} were calculated relative to the strongest 6117-keV and 6287-keV decays, respectively, for which HF$_\alpha$ = 1 was assumed. For the values that were not measured in this work, or for which more precise data exist in the literature, the references are given to the original studies. Simplified decay schemes of ^{175,177}Au and of ^{172}Ir are taken from [16] and [9], respectively. The new α-branching ratio of ^{172}Ir^{hs} was deduced in this work, see text. A value of $\Delta 2 = 207(14)$ keV for ^{175}Au^{hs} was quoted in [8]. The relative positions of the α-decaying states in ^{176}Au, ^{172}Ir, and ^{168}Re are not experimentally known. The respective decay schemes of ^{172}Ir^{ls,hs} are shown in the same way as given in the original work [9], apart of the new data or interpretation from the present work, see text.

Furthermore, as seen from Fig. 1(b), both the broad structure at 6060–6160 keV and the peak at 6222 keV observed in Fig. 1(c) are in coincidence with the Ir $K_{\alpha,\beta}$ x rays. The 6222 keV peak is readily understood as due to the α-e^-(K shell) summing in the PSSD of the energies of the 6082 and/or 6117 keV α decays with the energies of the internal conversion electrons resulting from the K-shell conversion of the coincident 175.2 and 211.6 keV γ transitions. As shown in the following section, both γ rays should be of a dominant $M1$ multipolarity, with respective theoretical K-shell conversion coefficients of $\alpha_K(175.2, M1) = 1.03$ and $\alpha_K(211.6, M1) = 0.61$ [23] and K-shell conversion electrons energies of $E_K(175.2) = 99$ keV and $E_K(211.6) = 135$ keV. Such an effect is well known in experiments at the recoil separators such as SHIP, when the recoils are implanted at a depth of a few μm in a silicon detector, see, e.g., [17,18]. The summing nature of the 6222 keV peak is also confirmed by Fig. 1(d), which shows the results of the GEANT Monte Carlo simulations with the dedicated code developed for the SHIP detection system [18]. The assumptions used in the simulations and a detailed discussion of results will be given in Sec. III B. We note that the study [7] also suggested this effect as the possible reason for their 6220 keV peak.

The 6287-keV decay is readily assigned as the full energy direct decay between the high-spin isomers in ^{176}Au and ^{172}Ir. Importantly, the 6287-keV peak in in Fig. 1(c) is approximately 1.7 times less intense than the 6222 keV peak, while in Fig. 1(a) the 6287 keV peak is much stronger. This proves that the 6827 keV peak in Fig. 1(a) consists of two contributions with similar energies, which must then originate from both isomers in ^{176}Au. We shall return to this discussion in Sec. III C.

A relative intensity of 8(1)% was deduced for the 6287 keV decay of the hs isomer by comparing its intensity in Fig. 1(c) with the intensity of all α decays in the region of 6060–6300 keV. The intensities of the 6082 and 6117 keV decays of ^{176}Au^{hs} will be discussed in the next section, as their evaluation depends on the assumed multipolarity (thus, conversion coefficients) of the 175 and 212 keV γ-ray transitions.

No clear evidence was found in the α_1(^{176}Au)-α_2(5510 keV, ^{172}Ir^{ls}) correlation analysis with the 5510-keV α decay of the 4.4(3) s low-spin isomer in ^{172}Ir [9]. This result agrees with the

low α-decay branching ratio of $b_\alpha \sim 2\%$ proposed for ^{172}Ir^{ls} in [9], which is beyond the sensitivity of this measurement.

B. Multipolarities of the observed γ decays of ^{172}Ir and GEANT simulations

For the discussion in this section, all measured γ-ray intensities from Figs. 1(b) and 2(a) were corrected for the respective γ-ray efficiencies from the work [13] and for internal conversion as described below. Since all α-γ coincidences attributed to ^{176}Au in Figs. 1(b) and 2 were observed within a short time interval of $\Delta T(\alpha\text{-}\gamma) \leqslant 500$ ns, the multipolarities of the corresponding γ rays in the daughter ^{172}Ir must be limited to $E1$, $M1$, $E2$, or $M2$. In some cases, a more precise multipolarity determination can be done by comparing the number of Ir $K_{\alpha,\beta}$ x rays in Figs. 1(b) and 2 with the numbers of coincidences for the six α-γ groups attributed to ^{176}Au, and making specific assumptions on the possible multipolarity (thus, conversion) of the respective γ rays.

Due to their low intensities no definitive conclusion can be drawn on the possible multipolarity of the four weakest 126.3, 151.5, 236.6, and 500.0 keV transitions. However, even by assuming the *largest* allowed $M2$ multipolarity for all four decays, the contribution of their K-shell internal conversion to Ir $K_{\alpha,\beta}$ x rays in Fig. 2(a) cannot exceed 25%. On these grounds we can safely conclude that the Ir $K_{\alpha,\beta}$ x rays in Figs. 1(b) and 2 must predominantly originate from the K-shell conversion of either 175.2 keV or 211.6 keV γ rays, or from both of them.

Furthermore, we can safely rule out an $M2$ multipolarity for the 175.2 keV transition. This is because, based on the number of the 6117–175.2 keV decays in Fig. 2(a) and by using the theoretical K-shell internal conversion coefficient of $\alpha_K(M2, 175.2\ \text{keV}) = 5.1$ [23], the expected number of the Ir K x rays due to this transition alone would be a factor of $\sim$4 larger than their *total* number in Fig. 2(a).

By applying the same method and assuming an $M2$ multipolarity ($\alpha_K(M2, 211.6\ \text{keV}) = 2.67$ [23]) for the 211.6-keV γ ray, the expected number of the Ir K x rays due to this decay alone is practically the same, within statistical uncertainty, as their total number in Fig. 2(a). In other words, under this assumption, all observed Ir K x rays would originate from the 211.6-keV decay alone, which is a highly unlikely scenario. This scenario would also require an $E1$ multipolarity for the 175.2-keV γ ray, as any other multipolarity for this decay would result in an excess of expected total number of Ir K x rays over the observed number. Based on the above arguments, we exclude an $M2$ multipolarity for the 211.6-keV γ ray.

On the other hand, by assuming an $M1$ (or possibly, a weakly mixed $M1 + E2$) multipolarity for both 175.2 and 211.6 keV decays, we can *simultaneously* describe the total number of registered α decays of ^{176}Au^{hs}, the α-decay intensity pattern in Fig. 1(c) and the γ-ray intensity pattern in Fig. 2(a). In this case, both decays are relatively strongly K-shell converted [$\alpha_K(175.2) = 1.03, \alpha_K(211.6) = 0.61$] [23], which will lead to the strong α-e^- summing peak at 6222 keV as mentioned earlier.

This analysis is complicated by the fact that the true intensity ratio between the 6082 keV and 6117 keV decays could only be established if the experimental internal conversion coefficients for the 175.2 and 211.6 keV decays were known, which is not the case in our study. Furthermore, the α-e^- summing in the PSSD results in an overlay of two contributions due to summing in the $\alpha(6082) + e^-$ and $\alpha(6117) + e^-$ branches.

Therefore, to shed more light on the decay pattern of ^{176}Au^{hs} we carried out GEANT Monte Carlo simulations with the dedicated code, developed for the SHIP detection system [18]. Due to an incomplete knowledge of some of the necessary parameters of the decay scheme, e.g., the degree of the $M1 + E2$ mixing, we did not aim at an exact reproduction of all features in the spectra. Rather, we aimed to describe the most prominent α-decay peaks, their shapes and relative intensities, as seen in Fig. 1(c). In particular, a special attention was paid to the correct reproduction of the intensity ratios between the α-e^- summing peak at 6222 keV and both the 6287 keV decay and the two-peak structure due to the 6082–6117 keV decays, under an addition constraint of keeping the number of the expected Ir K x rays consistent with their number in Fig. 2(a). For the sake of simplicity of the analysis, only the K-shell internal conversion of the 175.2 and 211.6 keV decay was considered, as the L/M-shells conversion contributes at most $\sim$17% in the case of $M1$ decay. The resulting simulated spectrum for ^{176}Au^{hs} in Fig. 1(d) reproduces the experimental spectrum in Fig. 1(c) quite well and establishes the relative α-decay intensity pattern as shown in Fig. 3 and Table II. On these grounds, an $M1$ multipolarity (with possibly a weak $E2$ admixture) was assigned for both 175.2 and 211.6 keV transitions, while any other pure multipolarity combinations failed to reproduce either the α decay spectrum, or the γ decay spectrum, or both of them.

Finally, an $M1$ assignment for both 175.2 and 211.6 keV transitions rules out an $M2$ multipolarity for the 126.3 and 151.5-keV γ rays, otherwise the intensity balance for observed Ir K x rays would not be fulfilled. Thus, only $E1$, $M1$, and $E2$ multipolarities with relatively low conversion K-shell coefficients are possible for the 126.3 and 151.5 keV γ rays. Due to their low intensities, the 236 and 500 keV γ rays will not change the intensity balance irrespectively of their multipolarity, including the maximum allowed $M2$. Therefore, the upper limits of the intensities for the respective coincident α decays were estimated by assuming an $M1$ multipolarity for the 126.3, 151.5, 236.6, and 500.0 keV transitions. Furthermore, an upper limit of the total number of fine-structure α decays of ^{176}Au^{ls} (thus excluding the 6287 keV decay) was estimated, which will be used in the next section to deduce relative intensities of fine-structure α decays of ^{176}Au^{ls}, quoted in Table II.

C. Intensity of α decay of ^{176}Au^{hs,ls} and α-decay branching ratio of ^{172}Ir^{hs}

A total number of $N_\alpha(^{176}\text{Au}^{hs}) = 1.2(1) \times 10^5$ of α decays of the high-spin isomer in ^{176}Au was deduced based on the number of $\alpha(6082)$-$\gamma(211.6)$ and $\alpha(6117)$-$\gamma(175.2)$ coincidences in Fig. 2(a), attributed to this isomer. The necessary

corrections for the γ-ray efficiency and internal conversion for the pure $M1$ 175.2 and 211.6 keV transitions were implemented in this analysis. We note that that in case of weakly mixed $M1 + E2$ nature of one (or both) of these transitions, a slightly reduced value of $N_\alpha(^{176}\mathrm{Au}^{\mathrm{hs}})$ will result due to slightly smaller conversion coefficients, which will however not change any of our inferences, see below.

The α-decay branching ratio of $^{172}\mathrm{Ir}^{\mathrm{hs}}$ was deduced by two *independent* methods by using the relation $b_\alpha(^{172}\mathrm{Ir}^{\mathrm{hs}}) = \frac{N_\alpha(^{172}\mathrm{Ir}^{\mathrm{hs}})}{N_\alpha(^{176}\mathrm{Au}^{\mathrm{hs}})}$, where $N_\alpha(^{172}\mathrm{Ir}^{\mathrm{hs}})$ is the number of α decays of $^{172}\mathrm{Ir}^{\mathrm{hs}}$ occurred in the experiment. The two methods differ in the ways in which the $N_\alpha(^{176}\mathrm{Au}^{\mathrm{hs}})$ and $N_\alpha(^{172}\mathrm{Ir}^{\mathrm{hs}})$ values were obtained.

In the first method, $N_\alpha(^{172}\mathrm{Ir}^{\mathrm{hs}})$ was determined from the number of $\alpha(5828)$-$\gamma(162.1)$ coincidences of $^{172}\mathrm{Ir}^{\mathrm{hs}}$ in Fig. 1(b), assuming a negligible direct production of ^{172}Ir in the $^{141}\mathrm{Pr}(^{40}\mathrm{Ca},\alpha 5n)^{172}\mathrm{Ir}$ reaction at the beam energies of 208 and 212 MeV. Indeed, the statistical model calculations with the HIVAP code [24] predict the cross-section ratio of $\sigma(5n)/\sigma(\alpha,5n) > 20$–$30$ at these beam energies. Therefore, essentially all ^{172}Ir present in our data was produced by α decay of the parent ^{176}Au. Based on the number of the α(5828 keV) -γ(162 keV) coincident decays of $^{172}\mathrm{Ir}^{\mathrm{hs}}$, normalized on the respective γ-ray efficiency and the total internal conversion coefficient of the 162.1 keV decay ($\alpha_{\mathrm{tot}} = 0.99(9)$, [23]), a value of $N_\alpha(^{172}\mathrm{Ir}^{\mathrm{hs}}) = 1.2(2) \times 10^4$ could be deduced from our data. We note that the above-quoted conversion coefficient for the 162.1 keV transition was taken from [23] to reproduce the experimentally measured K-shell conversion coefficient of $\alpha_K = 0.69(6)$ from Ref. [9], which corresponds to the mixed $48\%M1 + 52\%E2$ multipolarity for this transition. Finally, by comparing the $N_\alpha(^{176}\mathrm{Au}^{\mathrm{hs}})$ and $N_\alpha(^{172}\mathrm{Ir}^{\mathrm{hs}})$ values given above, a value of $b_\alpha(^{172}\mathrm{Ir}^{\mathrm{hs}}) = 10(2)\%$ was deduced.

Importantly, this method relies only on the ratio of the same type of events (α-γ coincidences) for the parent $^{176}\mathrm{Au}^{\mathrm{hs}}$ and daughter $^{172}\mathrm{Ir}^{\mathrm{hs}}$ nuclides, measured with the same set of detectors and in the same geometry for both nuclei. Furthermore, the similarity of the γ rays energies and multipolarities for both nuclei ensures that no substantial systematic uncertainty is introduced in this method due to the correction for the γ-ray efficiency and internal conversion.

The second method is based on α-α correlation analysis for the summing $\alpha + e^-$ peak at 6222 keV in Fig. 1. In this case, the value of $N_\alpha(^{172}\mathrm{Ir}^{\mathrm{hs}})$ can be reliably deduced from the number of $\alpha_1(6222)$-$\alpha_2(5822)$ correlations from Fig. 1(c), corrected for the correlation efficiency for α decays. On the other hand, the number $N_\alpha(^{176}\mathrm{Au}^{\mathrm{hs}})$ can be deduced from Fig. 1(b), by using the number of coincident $\alpha(6222)$-Ir $K_{\alpha,\beta}$ x rays, after correction for the γ-ray detection efficiency.

By using this method, an α-branching ratio of $b_\alpha(^{172}\mathrm{Ir}^{\mathrm{hs}}) = 9(1)\%$ was deduced, which is in a good agreement with the branching ratio obtained above by using α-γ data only. Furthermore, based on the total number of correlated α decays in the energy interval of 6000–6320 keV in Fig. 1(c), after the corrections for $b_\alpha(^{172}\mathrm{Ir}^{\mathrm{hs}}) = 9(1)\%$ and PSSD efficiency, a total number $N_\alpha = 1.0(1)\times 10^5$ of α decays of $^{176}\mathrm{Au}^{\mathrm{hs}}$ was deduced, which is in a good agreement with the value deduced from the α–γ analysis above.

As the two methods are independent, we combined two deduced values in our final value of $b_\alpha(^{172}\mathrm{Ir}^{\mathrm{hs}}) = 9.5(11)\%$ and the total intensity $N_\alpha(^{176}\mathrm{Au}^{\mathrm{hs}}) = 1.1(1)\times 10^5$. Our α-decay branching ratio is more than a factor of two lower than the value of $b_\alpha(^{172}\mathrm{Ir}^{\mathrm{hs}}) = 23(3)\%$ reported in [9].

Finally, the amount of 6287 keV decays of $^{176}\mathrm{Au}^{\mathrm{hs}}$ in the "combined" peak at 6287 keV in Fig. 1(a) can be estimated from the number of correlated $\alpha_1(6287)$–$\alpha_2(5822)$ decays from Fig. 1(c), corrected for our α-branching ratio of $^{172}\mathrm{Ir}^{\mathrm{hs}}$, "beam off/total" ratio and PSSD efficiency. Based on this analysis, we conclude that only $\sim$15% of the total intensity of the 6287 keV peak in Fig. 1(a) originates from $^{176}\mathrm{Au}^{\mathrm{hs}}$, while the dominant contribution must be attributed to the decay of the low-spin isomer $^{176}\mathrm{Au}^{\mathrm{ls}}$. Together with the intensity of four weaker α decays of $^{176}\mathrm{Au}^{\mathrm{ls}}$ estimated in the previous section, the total intensity of α decays of $^{176}\mathrm{Au}^{\mathrm{ls}}$ observed in our experiment is $N_\alpha(^{176}\mathrm{Au}^{\mathrm{ls}}) = 5.5(4)\times 10^4$. This allows the relative intensities of fine-structure α decays of $^{176}\mathrm{Au}^{\mathrm{ls}}$ to be determined, which are quoted in Table II. As only the upper limits for the the intensities of the fine-structure α decays of $^{176}\mathrm{Au}^{\mathrm{ls}}$ could be derived, their intensities are given relative to the strongest 6287 keV decay of this isomer.

IV. DISCUSSION

A. General systematics of the multiplet states in ^{176}Au, ^{172}Ir and in ^{168}Re

Spectroscopic studies of the odd-odd gold, iridium, and rhenium isotopes are difficult as even at low excitation energy the level density can be relatively high due to the coupling between different valence protons and neutrons. An inspection of the Nilsson diagrams in Fig. 4 shows that the interpretation of the states in ^{176}Au ($N = 97$, $Z = 79$), ^{172}Ir ($N = 95$, $Z = 77$), and ^{168}Ir ($N = 93$, $Z = 75$) is complicated by the close proximity to the respective Fermi surfaces and a near-degeneracy of the $\pi 3s_{1/2}$, $\pi 2d_{3/2}$, and $\pi 1h_{11/2}$ proton orbitals on the one hand and of the $\nu 1h_{9/2}$ and $\nu 2f_{7/2}$ neutron orbitals on the other. Therefore, the first step in our discussion is the inspection of the known low-lying states in the neighboring odd -A ^{175,177}Au and ^{171,173}Ir isotopes, which could provide direct information on the lowest proton configurations expected in ^{176}Au and ^{172}Ir. The simplified α-decay schemes of these odd -A nuclei, compiled from [3,9,25,26], are shown in Fig. 3 on the left and on the right hand sides of the decay scheme of $^{176}\mathrm{Au}^{\mathrm{hs,ls}}$ deduced in our work.

The known isomeric $11/2^-(\pi 1h_{11/2})$ excited states in ^{175,177}Au decay by unhindered α decay between the states of the same spin, parity and configuration, with typical reduced α widths $\delta_\alpha^2 \sim 50$–90 keV [3,9,26], see also Table II of [25] for several other cases of the $11/2^- \rightarrow 11/2^-\alpha$ decays in this region. Therefore, it is expected that the unique-parity $\pi 1h_{11/2}$ configuration should play an important role for the high-spin isomer in ^{176}Au and its daughter products.

The situation with the low-spin states in ^{176}Au and its daughters is more uncertain. This is because ^{176}Au lies in the middle of the transitional region between possibly weakly deformed or triaxial isotopes ^{177,179}Au on the one hand and presumably nearly spherical isotopes ^{171,173,175}Au on the other.

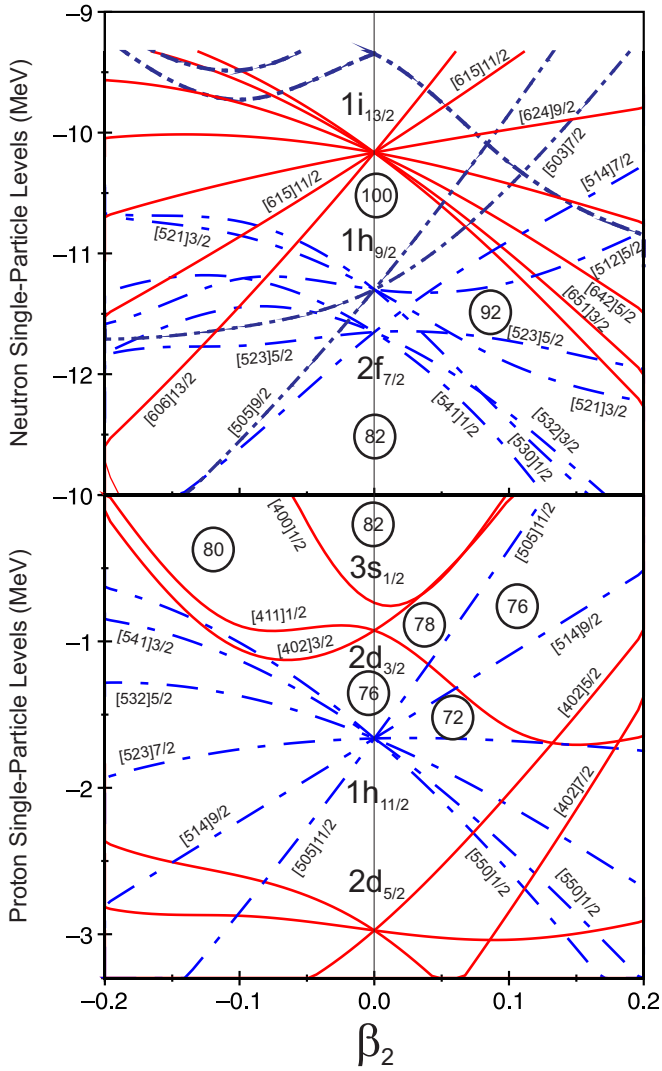

FIG. 4. (Color online) Nilsson orbitals, relevant for the region of ^{176}Au and ^{172}Ir, calculated with a Woods-Saxon potential [27]; top: for neutrons and bottom: for protons.

The $I^\pi = (1/2^+)$ ground states of ^{171,173,175}Au were proposed as being due to the $1/2^+[400]\pi 3s^{-1}_{1/2}$ proton configuration, see, e.g, [3,25], though the admixture of $\pi 2d_{3/2,5/2}$ should also be expected. As stated in [3] for ^{177}Au: "...Given the distribution of single-particle states near the proton Fermi surface and the limited decay information available on the daughter ^{173}Ir and parent ^{181}Tl nuclei, a tentative $(1/2^+, 3/2^+)$ assignment is proposed for the isomer in ^{177}Au. The most likely configuration is either $1/2^+[411](d_{3/2})$ at oblate deformation, or $3/2^+[402](d_{3/2})$ at prolate deformation, albeit some $s_{1/2}$ admixture should also be expected". However, the recent study of hyperfine splitting of atomic levels in ^{177}Au at ISOLDE (CERN) [28] strongly suggests the spin-parity assignment of $(1/2^+)$ for this nucleus. Nevertheless, the deduced magnetic moment for this state clearly deviated from the well-established systematics of the magnetic moments for a presumably pure $s_{1/2}$ proton orbital in odd -A Tl isotopes. This suggests that this state in ^{177}Au either indeed originates from a different orbital, e.g., $d_{3/2}$ or has a mixed $d_{3/2}/s_{1/2}$ character. This issue will be discussed elsewhere [29].

Due to the close proximity of two neutron $\nu 1h_{9/2}$ and $\nu 2f_{7/2}$ neutron subshells, see Fig. 4 , an even more complex situation is expected for the neutron configurations in ^{176}Au and in ^{172}Ir. In the literature, see, e.g., [7,9], several different neutron configurations were proposed for these nuclei, such as $7/2^-[503]$, $7/2^-[514]$, $5/2^-[512]$, $5/2^-[523]$, $3/2^-[521]$, all of them of mixed $\nu 1h_{9/2}/\nu 2f_{7/2}$ origin, depending on the sign and degree of deformation, which are yet unknown experimentally. Total Routhian surface calculations were performed in [7] for ^{176}Au, which also tried to account for possible triaxiality of this nucleus. However, in our opinion, due to the lack of experimental data on deformations and the variety and complexity of possible configurations, any such calculations will be highly tentative and it is practically impossible at present to unambiguously determine their specific neutron configurations.

To conclude this qualitative discussion, we mention that the study [7] proposed a $I^\pi = (3^-)$ assignment for this isomer, while in the most recent study of ^{176}Au at FMA [8], a spin-parity of (4^-) and a $\pi 1/2^+(s_{1/2}) \otimes \nu 7/2^-(h_{9/2}/f_{7/2})$ configuration were tentatively suggested. While our analysis supports this configuration assignment, we presently prefer to keep both $(3^-,4^-)$ options, which are possible for this proton-neutron multiplet, see Fig. 3.

The high-spin isomer in ^{176}Au would then most probably have a $I^\pi = (8^+,9^+)$ assignment due to the $\pi 11/2^-(h_{11/2}) \otimes \nu 7/2^-(h_{9/2}/f_{7/2})$ configuration, as shown in Fig. 3. The study [7] proposed a $I^\pi = (9^+)$ assignment for this isomer.

Important for the present discussion is also information on the spin and configuration assignments of the isomers in the daughter isotope ^{172}Ir^{hs,ls}. Here we refer the reader to the most detailed α- and β-decay studies of ^{172}Ir to date [9], which proposed two isomeric states with the tentative spins of (7^+) and (3^+). Another though less-detailed β-decay work [30] proposed a range of spins $(5^+,6^+)$ and (2,3) for the two isomers in ^{172}Ir.

B. Reduced α-decay widths for ^{176}Au^{hs,ls}

1. ^{176}Au^{hs}

With the aim to shed more light on the possible spin-parity assignments for ^{176}Au^{hs,ls} and its daughters, we now analyze the reduced α-decay widths, δ^2_α, for respective decays in the ^{176}Au$^{hs,ls} \rightarrow {}^{172}Ir^{hs,ls} \rightarrow {}^{168}$Re^{hs,ls} chains, see the middle panel of Fig. 3. The δ^2_α values have been calculated by using the Rasmussen approach [31] and assuming $\Delta L = 0$ decays.

Based on the unhindered nature of the 6082 and 6117 keV α decays of ^{176}Au^{hs} the 212 and 175 keV states most likely have a spin-parity of $I^\pi = (8^+,9^+)$ with the same proton-neutron configuration as the parent ^{176}Au^{hs} state. In contrast, the strong hindrance of ~40(6) for the 6287 keV decay indicates the clear difference between the configuration of ^{176}Au^{hs} and of the high-spin isomeric state in ^{172}Ir fed by the 6287 keV decay and by the 175 and 212 keV γ-ray transitions (the state which further decays by the 5828 keV α decay). Earlier, a tentative spin of $I^\pi = (7^+)$ and a $\pi 11/2^-[505](h_{11/2}) \otimes \nu 3/2^-[521](h_{9/2}/f_{7/2})$ configuration

were proposed for ^{172}Ir^{hs} [9]. The change of the neutron configuration between ^{176}Au^{hs} and ^{172}Ir^{hs} indeed seems to be the most plausible explanation for the hindrance of the 6287-keV α decay. The unhindered (or only weakly hindered) nature of the 5828 keV α decay from ^{172}Ir^{hs} establishes the same spin of (7^+) and configuration for the excited state at 162 keV in ^{168}Re^{hs}. As further suggested in [9] the subsequent 162 keV $M1/E2$ transition proceeds to the $I^\pi = (6^+)$, $\pi 9/2^-[514](h_{11/2}) \otimes \nu 3/2^-[521](h_{9/2}/f_{7/2})$ state in ^{168}Re, see Fig. 3.

In our opinion, the proposed configurations and a range of spin assignments (all tentative) fit well all known decay properties (including, β decay for ^{172}Ir^{hs} [9]) in the whole decay chain ^{176}Au^{hs} $\rightarrow$^{172}Ir^{hs} $\rightarrow$^{168}Re^{hs}. However, the reader must keep in mind a large variety of different configurations which are possible in these nuclei. Therefore detailed investigations, especially the direct measurements of the spin and magnetic moment for some of the observed long-lived states, is needed before any further conclusions can be drawn.

2. ^{176}Au^{ls}

In contrast to the 6287 keV α decay of ^{176}Au^{hs}, the 6287 keV decay of the low-spin isomer is unhindered (or only weakly hindered), which establishes the same spin/parity and configuration for the isomeric state in ^{172}Ir, fed by this decay. Following the discussion in Sec. III A 2 and in [7,8], we suggest the spin of $(3^-,4^-)$ and a $\pi 1/2^+(3s_{1/2}) \otimes \nu 7/2^-(h_{9/2}/f_{7/2})$ configuration to both states, see Fig. 3. We note that the present assignment differs from the proposed spin of (3^+) due to the assumed $\pi 11/2^-[505](h_{11/2}) \otimes \nu 5/2^-[523](h_{9/2}/f_{7/2})$ configuration in the study [9]. Furthermore, the assignment from [9] would be inconsistent with the $(4^-,5^-)$ spin, proposed for ^{180}Tl [8,21].

The unhindered nature of the 5510 keV α decay of ^{172}Ir^{ls} establishes the same configuration and a range of $I^\pi = (3^-,4^-)$ for the excited state fed by this α decay [9], however the exact γ-decay sequence of this excited state is not known. Indeed, the study [9] established the presence of three γ decay at 89.7, 123.2 ($E1$) and 136.3 keV in coincidence with the 5510 keV α decay, but no conclusion was drawn on their relative sequence. We note that an attempt to interpret the available data was undertaken in the evaluation [15], but in our opinion, it is highly tentative due to incompleteness of the measured data. Due to this, in Fig. 3 we reproduce the respective decay scheme of ^{172}Ir^{ls} in the same way as it was shown in the original work [9]. The remaining four weak α decays of ^{176}Au^{ls} are all hindered to some degree, but the absence of the multipolarity assignments for the respective coincident γ decays prohibits us from drawing any conclusions on the nature of the states at 126, 152, 237, and 500 keV.

V. CONCLUSIONS

The α-decay study of the isotope ^{176}Au was performed in the complete fusion reaction of ^{40}Ca ions with the ^{141}Pr target. To our knowledge, this is the most detailed study up to date, with statistics at least an order of magnitude higher than in any previous investigations of this isotope. The complex decay scheme of two isomers in this nuclide was established, including several weak fine-structure α decays. Multipolarities for the 175-keV and 212-keV γ-ray transitions and a new α-decay branching ratio were deduced for the high-spin isomer in ^{172}Ir. The dedicated measurements of spins and magnetic moments are needed to better understand the structure of the isomeric states in ^{176}Au^{hs,ls} and ^{172}Ir^{hs,ls}, these experiments are currently in preparation by our collaboration.

ACKNOWLEDGMENTS

We thank the UNILAC staff for providing the stable and high intensity ^{40}Ca beams. This work was supported by FWO-Vlaanderen (Belgium), by GOA/2010/010 (BOF KU Leuven), by the IAP Belgian Science Policy (BriX network P7/12), by the European Commission within the Seventh Framework Programme through I3-ENSAR (contract no. RII3-CT-2010-262010), by a grant from the European Research Council (ERC-2011-AdG-291561-HELIOS), by the United Kingdom Science and Technology Facilities Council (STFC), by the Slovak grant agency VEGA (Contracts No. 1/0576/13 and 2/0121/14), by the Slovak Research and Development Agency (Nos. APVV-0105-10 and APVV-0177-11) and by the Reimei Foundation of Advanced Science Research Center (ASRC) of JAEA (Tokai, Japan)

[1] J. Van Maldeghem and K. Heyde, Fizika **22**, 233 (1990).
[2] K. Heyde and J. L. Wood, Rev. Mod. Phys **83**, 1467 (2011).
[3] F. G. Kondev *et al.*, Phys. Lett. B **512**, 268 (2001).
[4] C. Cabot *et al.*, Nucl. Phys. A **241**, 341 (1975).
[5] J. Schneider, PhD thesis, GSI-report GSI-84-3, 1984 (unpublished).
[6] M. W. Rowe *et al.*, Phys. Rev. C **65**, 054310 (2002).
[7] J. T. M. Goon, PhD thesis, University of Tennessee, Knoxville, 2004 (unpublished).
[8] F. G. Kondev *et al.*, EPJ Web of Conferences **63**, 01013 (2013).
[9] W.-D. Schmidt-Ott *et al.*, Nucl. Phys. A **545**, 646 (1992).
[10] G. Münzenberg *et al.*, Nucl. Instrum. Methods **161**, 65 (1979).
[11] A. N. Andreyev *et al.* (unpublished).
[12] S. Hofmann *et al.*, Z. Phys. A **291**, 53 (1979); S. Hofmann and G. Münzenberg, Rev. Mod. Phys. **72**, 733 (2000).
[13] F. P. Hessberger *et al.*, Eur. Phys. J. A **43**, 55 (2010).
[14] S. Saro *et al.*, Nucl. Instrum. Methods Phys. Res. A **381**, 520 (1996).
[15] Evaluated Nuclear Structure Data File (ENSDF), http://www.nndc.bnl.gov/ensdf/.
[16] A. N. Andreyev *et al.*, Phys. Rev. C **80**, 024302 (2009).
[17] F. P. Hessberger *et al.*, Nucl. Instrum. Methods Phys. Res. A **274**, 522 (1989).
[18] A. N. Andreyev *et al.*, Nucl. Instrum. Methods Phys. Res. A **533**, 409 (2004).

[19] R. B. Firestone *et al.*, *Table of Isotopes*, 8th ed. (John Wiley and Sons, Inc., New York/Chicester/Brisbane/Toronto/Singapore, 1996).
[20] A. N. Andreyev *et al.*, Phys. Rev. Lett. **105**, 252502 (2010).
[21] J. Elseviers *et al.*, Phys. Rev. C **84**, 034307 (2011).
[22] J. Elseviers *et al.*, Phys. Rev. C **88**, 044321 (2013).
[23] T. Kibédi *et al.*, Nucl. Instrum. Methods Phys. Res. A **589**, 202 (2008); conversion coefficients calculator BrIcc v2.2a, http://www.rsphysse.anu.edu.au/nuclear/bricc/.
[24] W. Reisdorf *et al.*, Z. Phys. A **342**, 411 (1992).
[25] G. L. Poli *et al.*, Phys. Rev. C **59**, R2979 (1999).
[26] A. N. Andreyev *et al.*, Phys. Rev. C **87**, 054311 (2013).
[27] S. Cwiok, J. Dudek, W. Nazarewicz, W. Skalski, and T. Werner, Comp. Phys. Comm. **46**, 379 (1987).
[28] IS534 experiment at ISOLDE, http://cds.cern.ch/record/1551259/files/INTC-P-319-ADD-1.pdf.
[29] A. N. Andreyev *et al.* (unpublished).
[30] A. Bouldjedri *et al.*, Z. Phys. A **342**, 267 (1992).
[31] J. O. Rasmussen, Phys. Rev. **113**, 1593 (1959).